

Cyclic Electron Transfer in *Helicobacillus mobilis* Involving a Menaquinol-Oxidizing Cytochrome *bc* Complex and an RCI-Type Reaction Center[†]

David M. Kramer,^{*,‡,§} Barbara Schoepp,^{||} Ursula Liebl,[⊥] and Wolfgang Nitschke^{||,⊥}

Institute of Biological Chemistry, Washington State University, 289 Clark Hall, Pullman, Washington 99164-6340, Institut de Biologie Physico-Chimique, Service de Photosynthèse, 13, rue Pierre et Marie Curie, 75005 Paris, France, Biologisches Institut II, University of Freiburg, Schänzlestrasse 1, 79104 Freiburg, FRG, and BIP/CNRS, UPR 9036, Institut de Biologie Structurale et Microbiologie, 31 chemin Joseph Aiguier, 13402 Marseille Cedex 20, France

Received September 5, 1996; Revised Manuscript Received February 12, 1997[®]

ABSTRACT: Flash-induced absorption changes arising from *b*-type hemes were studied on whole cells of *Helicobacillus mobilis* under physiological and redox-controlled conditions. The sensitivity of the monitored redox changes to inhibitors of cytochrome *bc* complexes and the redox potential dependence of reduction and oxidation reactions of cytochrome *b*-hemes demonstrate that the respective *b*-hemes are part of a cytochrome *bc* complex. Both the half-time and the extent of flash-induced reduction of cytochrome *b* titrated with apparent potentials of about −60 and −50 mV (both *n* = 2), respectively, i.e., close to the $E_{m,7}$ value of the menaquinone (MK) pool, indicating a collisional interaction between menaquinol and the Q_o site of the cytochrome *bc* complex. At strongly reducing ambient potentials (<−150 mV), a net flash-induced oxidation of *b*-hemes was observed in agreement with the $E_{m,7}$ values of the individual hemes of −90 mV (b_h) and −190 mV (b_l) determined in equilibrium redox titrations on membrane fragments. From the extent of photooxidized *b*- and *c*-type hemes as well as P_{798}^+ , a stoichiometry of 0.6–0.75 cytochrome *bc* complexes per photosynthetic reaction center was estimated. The kinetic behavior and also the energy profiles for Q-cycle turnover of the helicobacterial complex are compared to those of cytochrome *bc*₁ complexes from purple bacteria and of cytochrome *b₆f* complexes from chloroplasts.

The study of cytochrome *bc* complexes in prokaryotes has for a long time focused on the proteobacteria (formerly called “purple bacteria and relatives”, Stackebrandt et al., 1988) with their cytochrome *bc*₁ complex, and on the cyanobacteria with their cytochrome *b₆f* complex.¹ In terms of evolution, these two classes of eubacterial enzymes are closely related to the respective enzymes in mitochondria and chloroplasts [for reviews, see Gray and Daldal (1995) and Kallas (1994)]. Ubiquinone (UQ)² and plastoquinone (PQ), the physiological electron donors to cytochrome *bc*₁ and *b₆f* complexes,

respectively, are lipophilic derivatives of the benzoquinone moiety. UQ and PQ, although distinguished by different ring substituents, share very similar spectral and electrochemical properties and especially a common redox midpoint potential at pH 7.0 of around +100 mV (Rich & Bendall, 1983). The occurrence in the bacterial world of UQ or PQ is largely restricted to the proteo- and cyanobacteria, whereas the vast majority of eubacteria (and a large part of the archaeobacteria) use the significantly different menaquinone (MK) for the quinone pools of their electron transport chains (Collins & Jones, 1981). Chemically, menaquinones are derivatives of the naphthalene moiety and are characterized by a redox midpoint potential of around −60 mV (Kröger & Uden, 1985; Zannoni & Ingledew, 1985; Liebl et al., 1992), i.e., about 150 mV more negative than that of UQ and PQ. Cytochrome *bc* complexes operating in electron transport chains involving MK pools have for a long time attracted only scant attention (Knaff & Malkin, 1976; Zannoni & Ingledew, 1985). Recently, a more detailed investigation of one subgroup of the MKH₂-oxidizing cytochrome *bc* complexes, i.e., those found in species belonging to the Firmicutes (formerly called the “Gram-positive” phylum; Wayne et al., 1987), was initiated (Kutoh & Sone, 1988; Liebl et al., 1990, 1992; Nitschke & Liebl, 1992; Riedel et al., 1993). The results obtained so far show that these MKH₂-oxidizing cytochrome *bc* complexes have properties that differentiate them from their UQH₂ and PQH₂-oxidizing counterparts in proteo- and cyanobacteria.

The significant differences of the Firmicutes cytochrome *bc* complex with respect to protein composition (Yu et al., 1995; Sone et al., 1996), inhibitor sensitivity (Riedel et al., 1993), and the chemical nature and redox midpoint potentials

[†] Supported by the European Commission (EEC BIO2CT-930076 and ERBCHBGCT930253, W.N.), by a NATO/NSF postdoctoral fellowship (D.M.K.), and by the WSU Plant Biochemistry Research and Training Center (DOE DE-FG06-94ER20160, D.M.K.) and the USDA (D.M.K.).

* Author to whom correspondence should be addressed at the Institute of Biological Chemistry, Pullman, WA 11964-6340. Telephone: ++(509) 335-4964. Fax: ++(509) 335-7643. E-mail: dkramer@wsu.edu.

[‡] Washington State University.

[§] Institut de Biologie Physico-Chimique.

^{||} University of Freiburg.

[⊥] Institut de Biologie Structurale et Microbiologie.

[®] Abstract published in *Advance ACS Abstracts*, April 1, 1997.

¹ The terms *bc*₁ and *b₆f* complex will in the following exclusively be used for the purple bacteria/mitochondrial and cyanobacterial/chloroplast enzymes. The homologous complex in *H. mobilis* will be referred to as a “*bc*” complex to emphasize its unique features.

² Abbreviations: 2FeS, 2-iron-, 2-sulfur-containing redox-active cluster; DBMIB, dibromothymoquinone; $E_{m,x}$, midpoint potential at pH *x*; EPR, electron paramagnetic resonance; Fd, ferredoxin; LED, light-emitting diode; MK and MKH₂, menaquinone and menaquinol, respectively; P_{798} and P_{798}^+ , reduced and oxidized primary chlorophyll donor in the *Helicobacillus mobilis* reaction center, respectively; PQ and PQH₂, plastoquinone and plastoquinol, Q_B , quinone reductase site of photosystem II and bacterial photosynthetic reaction centers; Q_L , quinone reductase site of *bc* complex; Q_o , quinol oxidase site of *bc* complex; RC, reaction center; UQ and UQH₂, ubiquinone and ubiquinol, respectively.

of substrates (Nitschke et al., 1995a,b) might raise doubts whether these enzymes fulfill a functional role comparable to their counterparts in proteobacteria, mitochondria, cyanobacteria, and chloroplasts. Only limited data with respect to the functional properties of these enzymes have been presented so far (Kutoh & Sone, 1988; Liebl, 1993). *Heliobacteria* represent the only known photosynthetic species within the phylum of the Firmicutes. In photosynthetic organisms, the electron transport events can be triggered and synchronized by single-turnover actinic flashes of light. The *heliobacteria* thus provide a well-suited system for the study of the function of a cytochrome *bc* complex within an electron transfer chain based on a MK pool. We have, therefore, studied the *in vivo* electrochemical and kinetic parameters of the cytochrome *bc* complex of *Heliobacillus mobilis*. The relative stoichiometries of the cytochrome *bc* complex and some of its electron transport partners have been estimated, and a tentative model of the photoinduced cyclic electron transport chain in *heliobacteria* is proposed. Implications of this model for the comparative bioenergetics of cytochrome *bc* complexes are discussed.

EXPERIMENTAL PROCEDURES

Cultures of *H. mobilis* [kindly provided by Drs. M. Madigan (Carbondale, IL) and R. E. Blankenship (Tempe, AZ)] were grown as described by Liebl et al. (1990). Using 5% inocula, the cultures were found to achieve late logarithmic growth phase after about 1.5 days. At 2 days, the stationary growth phase was reached accompanied by the appearance of large numbers of lysed cells and rapid loss of photoinduced absorbance changes (in 2.5-day-old cultures, only 10% of the maximal signals observable after 1.5 days remained). All experiments on whole cells described in this work were therefore performed on cultures of 1.0–1.5 days of age [see also Nitschke et al. (1995b)]. In this time range, cultures showed an average OD₇₈₀ of 0.5 in the measuring cuvette (path length of 1.6 cm). The pH of the medium after 1.5 days of growth was between 6.9 and 7.0. Aliquots of cell suspensions were transferred via air-tight syringes from the rubber-stoppered culture bottles into the Ar-flushed cuvette compartment for measurements.

Flash-induced optical absorbance changes were measured in whole cells on a flash-kinetic spectrometer as described in Joliot et al. (1980) and in Joliot and Joliot (1984) and on a similar instrument described in Kramer (1990). Both instruments were fitted with anaerobic cuvettes which were flushed with water-saturated high-purity N₂ or Ar gas.

Equilibrium redox titrations on membranes were performed on a Shimadzu MPS2000 spectrophotometer fitted with an anaerobic redox cuvette as described in Dutton (1971). Redox titrations of kinetics were performed on the flash kinetic spectrophotometers described above. Ambient potentials (E_h) were measured by a bare platinum electrode versus a standard silver/silver chloride electrode and corrected to reflect standard hydrogen electrode (SHE) potentials. Redox titration of cells and membranes was performed under a flow of water-saturated Ar gas, in the presence of the redox mediators indicated under Results. In the case of whole cells, about 5 min was required to attain stable potentials. This measured ambient redox potential remained constant within ± 5 mV (with superimposable kinetic traces at all wavelengths measured) for up to 10 min, subsequently starting to drift, probably as a result of metabolic processes.

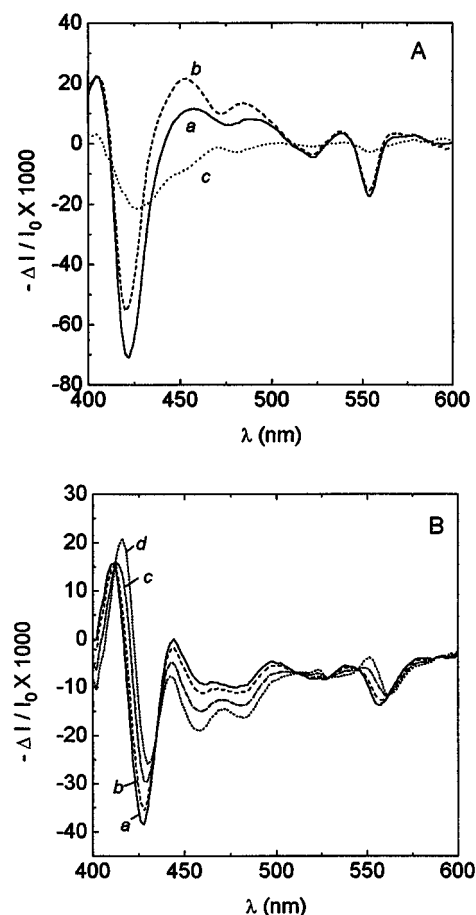


FIGURE 1: Light-induced redox changes in whole cells from *H. mobilis* recorded under anaerobic and aerobic conditions. (A) Trace *a* (solid line) represents a difference spectrum obtained by subtracting a spectrum taken after dark-adaptation under anaerobic conditions for at least 10 min (solid line) from a spectrum taken during illumination by red light (approximately $150 \mu\text{mol}$ of photons $\text{m}^{-2} \text{s}^{-1}$). In trace *b* (dashed line), the sample was aerated for 1 min, followed by dark base line and illuminated traces as above. Trace *c* (dotted line) represents the difference between traces *a* and *b*, or the difference in light-induced difference spectra taken under anaerobic and aerobic conditions. (B) Trace *a* represents the aerobic–anaerobic difference spectrum of whole cells of *H. mobilis* (conditions as in panel A). Traces *b*–*d* show the appearance of a *b*-type cytochrome spectrum after subtraction of contributions from *c*-type cytochromes as described in the text. The fraction of the representative *c*-type cytochrome spectrum subtracted from trace *a* was 0.1, 0.3, and 0.5 for traces *b*, *c*, and *d* respectively.

Saturating single-turnover flashes were obtained using lasers (ruby and/or Candela dye lasers) as described in Nitschke et al. (1995b) or xenon flashes as described by Kramer (1990).

DBMIB and stigmatellin were obtained from Sigma and Fluka, respectively.

RESULTS

Changes in the Redox States of Cytochromes Induced by Continuous Illumination in Vivo. Whole cells were allowed to dark adapt for 10 min and were then exposed to continuous red light (approximately $150 \mu\text{mol}$ of photons $\text{m}^{-2} \text{s}^{-1}$ 670 nm light from a LED). A light–dark difference spectrum of whole cells under anaerobic conditions (Figure 1A, trace *a*) was dominated by contributions from cytochromes that had become reduced by metabolic processes in darkness and that were transiently oxidized after the onset of continuous

illumination. After switching the continuous light off, the cells reversed to the dark-adapted state within about 5 min. The spectrum of the oxidized cytochromes is characterized by α -, β -, and γ -band bleedings at 553.5, 523, and 422 nm, respectively. The γ -band wavelength of 422 nm together with the long-wavelength isosbestic point of the γ -band at 441 nm was unusually high for a redox difference spectrum of *c*-type cytochromes (expected to be around 418 and 432 nm, respectively). This suggested that oxidized *b*-type hemes might contribute to the observed spectrum.

When cells were aerated for 1 min by bubbling air through the sample, a significantly different light–dark spectrum was obtained (Figure 1A, trace *b*). The extent of bleaching in the α -band region decreased by 15%, and the trough wavelength of the γ -band was shifted to 420 nm. Furthermore, the isosbestic point was observed at 434 nm, i.e., close to that expected for a pure *c*-type cytochrome. These changes in the light-induced difference spectrum indicate a relatively lower contribution from light-oxidized *b*-type hemes under aerobic conditions. The difference between the light–dark spectra in the aerobic and anaerobic states (Figure 1A, trace *c*) shows that both *c*-type and *b*-type hemes could be additionally oxidized by light in the anaerobic state.

This interpretation is substantiated by the dark difference spectrum between anaerobic and aerobic states (Figure 1B, trace *a*). This spectrum has broad α - and γ -band features (α -band peak at 556 nm with bandwidth of approximately 16 nm and γ -band peak at 427 nm with bandwidth of approximately 17 nm), suggesting that a significant amount of cytochrome *b* was oxidized by the introduction of air. Subtraction of various amounts of trace *b* of Figure 1A, which we assume to be largely due to oxidation of *c*-type cytochromes, resulted in red-shifting and narrowing of the α - and γ -bands of the aerobic–anaerobic difference spectrum (see Figure 1B, traces *b*–*d*), and the resulting curves strongly resemble the spectra of *b*-type cytochromes.

Time-Resolved Redox Changes of Hemes Induced by Single-Turnover Flashes Observed in Vivo. After a flash, photooxidized P_{798} was found to be re-reduced by a c_{553} -heme in several hundreds of microseconds, as described previously (Vos et al., 1989; Nitschke et al., 1995b) (data not shown). The oxidized heme was subsequently re-reduced in the several hundreds of milliseconds time range in whole cells under anaerobic conditions (see Figure 2A). During this re-reduction process, however, the γ -band peak wavelength shifted from 421 to 428 nm, indicating an oxidation of a *b*-type cytochrome concomitant with the reduction of cytochrome c_{553} (Figure 2A). Whereas in the spectral region of the γ -band contributions from cytochrome *b* and cytochrome *c* are strongly superimposed, there is only a small contribution from cytochrome *b* at the α -band wavelength of 553 nm. The kinetics at 553 nm together with the spectrum at 2.5 ms (which was essentially free of contributions from P_{798}^+ and cytochrome *b*) could therefore be used to subtract *c*-type cytochrome contributions from the spectra measured at longer times. Such a spectrum, obtained after subtraction of the contributions from photooxidized cytochrome c_{553} at 200 ms after the flash, is shown in Figure 2B. This spectrum corresponds to the oxidized minus reduced difference spectrum of a *b*-type cytochrome with no or only very low contributions from other spectral species, and is very similar to the dark difference spectrum between anaerobic and aerobic samples (Figure 1B). Its α -, β -, and

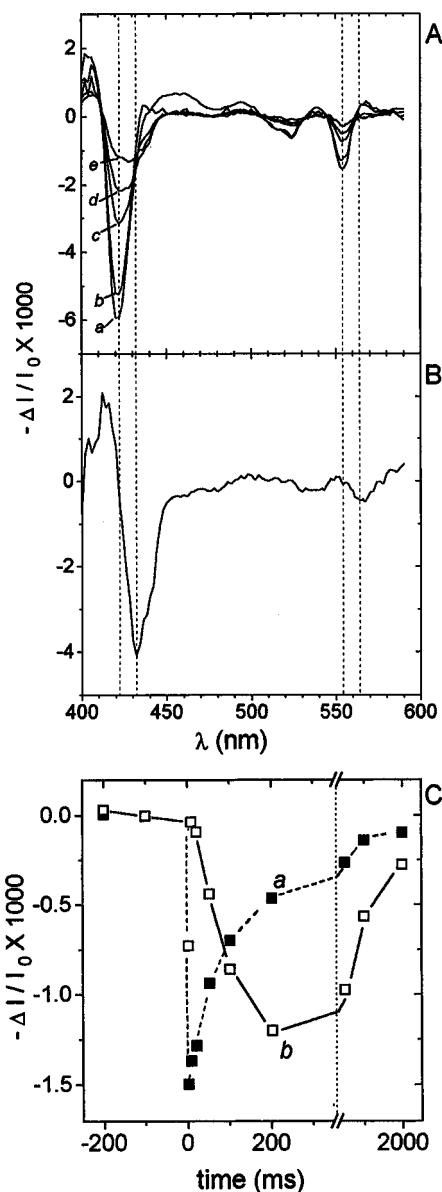


FIGURE 2: Time-resolved flash-induced absorbance spectra of anaerobic *H. mobilis* cells. Dark-adapted cells were illuminated at time zero with a saturating single-turnover laser pulse, and the light-induced absorbance changes were followed at wavelengths from 400 to 580 nm (see Experimental Procedures for details). (A) Traces *a*–*e* represent the absorbance spectra constructed from kinetic experiments at 2.5, 20, 100, 200, and 500 ms, respectively, after flash excitation. Panel B represents the spectrum of a *b*-type cytochrome obtained by subtracting contributions from *c*-type cytochromes from the time-resolved difference spectrum at 200 ms (see text for details). The dashed vertical lines in panels A and B are at approximately 421, 432, 554, and 564 nm. Panel C shows the kinetics of absorbance changes after flash excitation representative of redox changes in *c*-type cytochromes (553 nm, trace *a*, closed squares) and *b*-type cytochromes [$-\Delta I/I_{0\ 435\text{nm}} + 0.93(-\Delta I/I_{0\ 592\text{nm}})$, trace *b*, open squares].

γ -band maxima were found at 564 nm, between 530 and 535 nm and at 432 nm, respectively.

Since the γ -band maximum of this *b*-type cytochrome (432 nm) is close to the isosbestic points of the *c*-type cytochromes, well-resolved kinetic traces of the redox changes of cytochrome *b* can be obtained at wavelengths around 435 nm, at least at times longer than 2.5 ms, i.e., when contributions from P_{798}^+ have become negligibly small. Time-resolved spectra in the range between 400 and 480 nm were

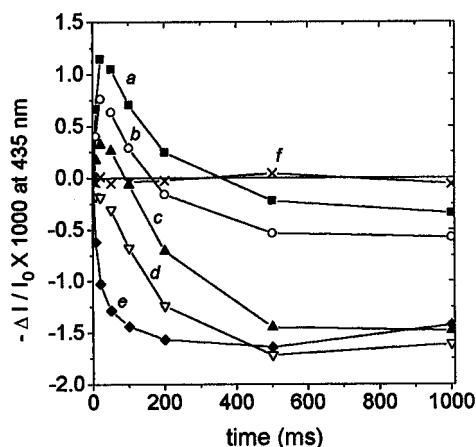


FIGURE 3: Flash-induced cytochrome *b* changes in *H. mobilis* cells at varying cellular redox states. Samples were aerated as in Figure 1A, and the flow of argon was reestablished to allow the redox potential of the cells to drop by metabolic processes. Single-turnover flash-induced absorbance changes at 435 nm, indicating changes in the redox state of *b*-type cytochromes at 1, 3, 5, 10, and 45 min under argon, are shown in traces *a–e*, respectively. Trace *f* shows the flash-induced 435 nm absorbance kinetics after 45 min under argon with the addition of 10 μ M stigmatellin to block the cytochrome *bc* complex.

recorded for all redox states discussed below (not shown), demonstrating that apart from *c*-hemes, *b*-hemes, and P_{798}^+ no other redox components measurably contributed to the absorption changes at 435 nm. From the data in Nitschke et al. (1995b), the absorbance change at 592 nm represents P_{798}/P_{798}^+ with practically no significant contributions from other species. Therefore, the kinetics of absorbance changes at 592 nm were scaled by -0.93 [i.e., the ratio of absorbance contributions of P_{798}/P_{798}^+ at 435 and 592 nm (Nitschke et al., 1995b)] and used to subtract out P_{798}/P_{798}^+ contributions from the 435 nm signals. With this procedure, cytochrome *b* redox kinetics could be resolved at times as short as 0.5 ms after a flash. A kinetic trace of cytochrome *b* redox changes measured in this way is shown in Figure 2c together with the kinetics of the *c*-type cytochrome measured at 553 nm. The oxidation of the *b*-heme is closely correlated to the rapid re-reduction phase of cytochrome c_{553} , indicating that the electrons re-reducing cytochrome c_{553} are ultimately provided by a process involving redox changes of cytochrome *b*. Assuming that the α - and γ -bands of cytochromes *b* and *c* have respectively similar extinction coefficients at their peaks, and that the γ -band absorbance change for cytochrome *b* at 435 nm is approximately 4-fold larger than at its α -band (see Figure 2B), it can be estimated that at 200 ms after the actinic flash 0.25 cytochrome *b* was oxidized for each cytochrome *c* re-reduced.

Aeration of the sample as described above resulted in a flash-induced absorption increase at 435 nm, indicating reduction of cytochrome *b* followed by a slow reoxidation on the order of hundreds of milliseconds (Figure 3, trace *a*). During the subsequent metabolism-induced decrease of the ambient redox potential within the cell, the extent of the reduction phase was attenuated, and a net oxidation of cytochrome *b* at long times was observed (Figure 3, traces *b–f*). After about 5 min of anaerobiosis, the transient reduction was replaced by a slow, nearly monotonic oxidation and the kinetics resemble those shown in Figure 2C. After extensive anaerobiosis, a more rapid cytochrome *b* oxidation phase ($t_{1/2}$ of about 6–8 ms) appeared.

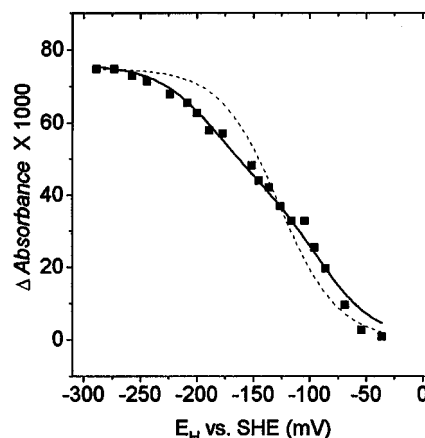


FIGURE 4: Equilibrium redox titration of *b*-type cytochromes in membrane fragments of *H. mobilis*. Membrane fragments of *H. mobilis* were prepared and placed in an anaerobic redox cuvette as described under Experimental Procedures with the following redox mediators (all at 5 μ M): 1,4-naphthoquinone, 5-hydroxy-1,4-naphthoquinone, duroquinone, 2,5-dihydroxy-*p*-benzoquinone, 2-amino-1,4-naphthoquinone, anthroquinone-1,5-disulfonate, and anthroquinone-2-sulfonate. Ambient potentials were adjusted as described under Experimental Procedures. Shown are the absorbance changes at 563 nm, after taking a base line between 545 and 575 nm (closed squares). The resulting titration data were fit to either one (solid line) or two (dashed line) $n = 1$ components. The one-component fit showed an E_m of -127 mV, while the two-component fit showed components of -92 and -186 mV.

Stigmatellin (10 μ M) and DBMIB (20 μ M) inhibited the described absorption transients at 435 nm under both aerobic and anaerobic conditions (see Figure 3 trace *f* for addition of 10 μ M stigmatellin under anaerobic conditions). This strongly suggests that the described *b*-type cytochromes are part of a cytochrome *bc* complex. A detailed description of the respective effects of various inhibitors on the *bc* complex will be published elsewhere.

Redox Titrations of Cytochrome *b* in Membrane Fragments. The *c*-type cytochromes in whole cells and membrane fragments from *H. mobilis* were found to titrate in the range of ambient potentials between $+250$ and -100 mV [see Nitschke et al. (1995b, 1996)]. Since the *b*-type hemes were found to be reduced only below -50 mV, their contributions could be subtracted out from the dominant *c*-type cytochromes, allowing reliable determination of signal intensities. The titration curves of the *b*-type heme α -peak measured at 563 nm are shown in Figure 4. The data were fit with either a single $n = 1$ species or the sum of two $n = 1$ species. The fit to one $n = 1$ component was poor, but a satisfactory fit was obtained with two $n = 1$ components, indicating the likely presence of two electrochemically distinct cytochrome *b* species with respective E_m values at approximately -92 and -190 mV. Within the noise level, the α -band absorbance spectra of the high- and low-potential components were indistinguishable (data not shown).

Redox Titration of the Flash-Induced Changes in the Redox State of Cytochrome *b*. Redox titrations were performed on cells using a cocktail of lipophilic, membrane-permeable mediators (see legend to Figure 5). At each stable potential, RC turnover was initiated by a short, saturating xenon flash, and the kinetics of cytochrome *b* were observed at $-\Delta I/I_{0,435\text{nm}} + 0.93(-\Delta I/I_{0,592\text{nm}})$.

At ambient redox potentials above $+50$ mV, a nearly constant level of flash-induced reduction of cytochrome *b* was observed (Figure 5A). The reduction kinetics under

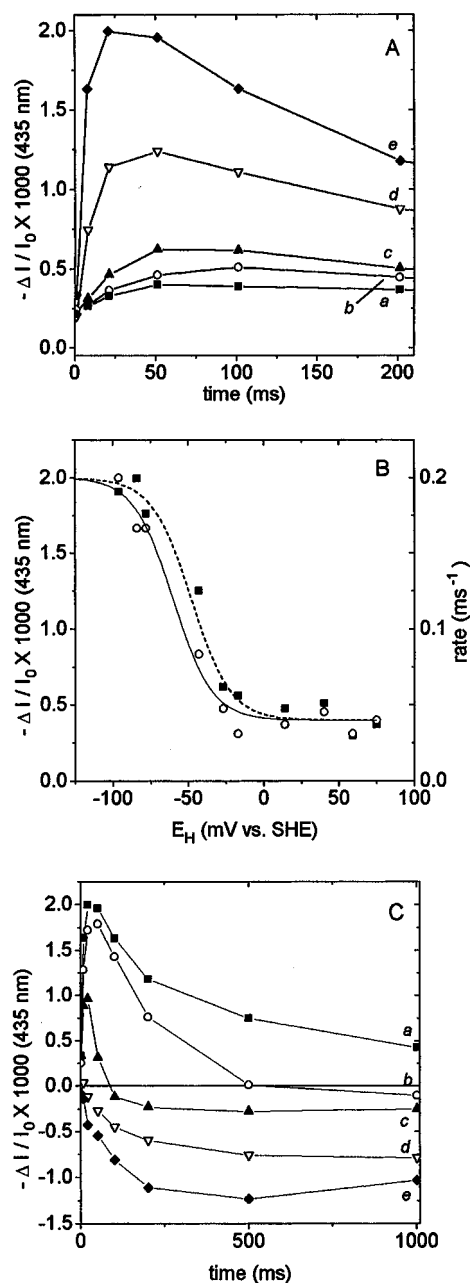


FIGURE 5: Redox titration of flash-induced cytochrome *b* redox changes in whole cells of *H. mobilis*. Cells were incubated in the dark under flowing argon gas with the following redox mediators (all at 500 nM): 2,5-dimethyl-*p*-benzoquinone, 1,2-naphthoquinone, 1,4-naphthoquinone, 5-hydroxy-1,4-naphthoquinone, duroquinone, 2,5-dihydroxy-*p*-benzoquinone, 2-amino-1,4-naphthoquinone, anthroquinone-1,5-disulfonate, and anthroquinone-2-sulfonate. Ambient potentials were adjusted as described under Experimental Procedures. After equilibration, single-turnover flashes were given, and the absorbance changes reflecting redox changes in *b*-type cytochromes [i.e., $-\Delta I/I_0(435\text{nm}) + 0.93(-\Delta I/I_0(592\text{nm}))$; see text] were recorded. High and low ambient potential traces are shown in panels A and C. In panel A, traces taken at 75 mV (trace *a*, closed squares), 40 mV (trace *b*, open circles), -27 mV (trace *c*, closed triangles), -43 mV (trace *d*, open triangles), and -84 mV (trace *e*, closed diamonds) are shown. Panel B represents the dependence of the extent (closed squares) and rate (open circles) of cytochrome *b* reduction on ambient redox potential. These curves were fit to the Nernst equation, yielding $n = 2$ titration curves with E_m values of -50 mV for the rate (dashed line) and -60 mV for the extent (solid line) of cytochrome *b* reduction. In panel C, kinetic traces taken at -84 mV (trace *a*, closed squares), -143 mV (trace *b*, open circles), -172 mV (trace *c*, closed triangles), -204 mV (trace *d*, open triangles), and -329 mV (trace *e*, closed diamonds) are shown.

these conditions were characterized by half-times in the range of 20–25 ms. Below 0 mV, both an acceleration and an increase in the extent of the reduction phase were observed (Figure 5A). At about -90 mV, the half-time for cytochrome *b* reduction reached a maximum of about 6 ms. In the region between +100 and -120 mV, the dependence on ambient redox potential of the extent of reduction and half-time could be described by $n = 2$ Nernst curves with E_m values of -50 and -60 mV, respectively (Figure 5B).

Below -100 mV, where significant chemical reduction of cytochrome *b_h* is expected in the dark (see Figure 4), the extent of flash-induced reduction of cytochrome *b* decreased, but the half-time for reduction remained constant (Figure 5C). At -172 mV, a small transient cytochrome *b* reduction, peaking at about 20 ms, was followed by a net oxidation.

At very low potentials (e.g., -329 mV), where both cytochromes *b_h* and *b_l* are expected to be fully reduced in the dark, a large oxidation of cytochrome *b* was observed with $t_{1/2}$ of 6–8 ms, following a short lag of about 0.5–1 ms. If a second flash was given approximately 200 ms after the first, a small transient cytochrome *b* reduction was followed by a further oxidation (not shown).

DISCUSSION

The presence of a cytochrome *bc* complex in heliobacteria was demonstrated by the detection of the characteristic EPR signal of the 2Fe2S cluster contained in cytochrome *bc* complexes, i.e., of the so-called Rieske center in *H. chlorum* (Liebl et al., 1990). Subsequently, this 2Fe2S cluster was studied in *H. mobilis* (Liebl, 1993), and its redox midpoint potential was determined to be +150 mV, a potential about 150 mV lower than those found for the 2Fe2S clusters in cytochrome *bc* complexes occurring in cyanobacteria and purple bacteria, but consistent with the presence of MK as the sole quinone redox carrier in heliobacteria (Hiraishi, 1989). In the present work, both the E_H dependence of redox changes of *b*-type cytochromes (e.g., reduction of *b*-hemes in the presence of MKH_2 induced by positive charges from P_{798}^+) and the effects of cytochrome *bc* inhibitors, characteristic for cytochrome *bc* complexes, demonstrate that the observed absorbance changes of *b*-type cytochromes arise from a cytochrome *bc*-type complex. The data obtained on whole cells in this work therefore provide insights concerning the function of this complex within the photosynthetic electron transfer chain of heliobacteria.

Cytochrome:RC Stoichiometries in *H. mobilis*. From the spectra shown in Figure 1A,B a stoichiometry of *c*-type hemes, *b*-type hemes, and RC was estimated. Assuming that all photooxidizable cytochrome *c* appears in the light–dark difference spectrum (anaerobic conditions, Figure 1A), and all oxidizable cytochrome *b* appears in the anaerobic–aerobic dark difference spectrum (Figure 1B), a ratio of cytochrome *b* to cytochrome *c* α -band absorbance extents is approximately 1:4. Assuming approximately equal extinction coefficients for cytochromes *b* and *c* at their respective α -bands, we obtained a ratio of 1 cytochrome *b* per 4 cytochrome *c* hemes photooxidized, or 1 *bc* complex per 8 cytochrome *c* hemes. Previously, a ratio of about 5–6 cytochrome *c* hemes per RC was determined (Nitschke et al., 1995b), yielding 0.6–0.75 cytochrome *bc* complexes per RC. A possible source of error could be that not all cytochromes were reduced in the anaerobic state in darkness.

This does not seem likely, however, since addition of 1 mM sodium dithionite at pH 7.0 in the presence of 5 μ M each of phenazine methosulfate and 1,2-naphthoquinone did not induce further reduction of cytochromes (not shown). A small amount of *c*-type cytochrome appears to have been oxidized upon aeration (Figure 1B). However, the fact that similar amounts of *c*-type cytochromes were photooxidized under both aerobic and anaerobic conditions (see above) suggests that the high-potential chain of redox components reached a similar oxidation state under constant illumination in both cases. The cytochromes oxidized upon addition of air may not be photooxidizable. The values given above represent a first approximation of the stoichiometries of some of the electron carriers in the *H. mobilis* electron transfer chain.

Electrochemical Potentials of the Redox Centers Contained in the Heliobacterial Cytochrome *bc* Complex. Equilibrium redox titrations on *H. mobilis* membranes show the presence of two, electrochemically-distinct cytochrome *b* species, with midpoint potentials of approximately -92 and -190 mV (Figure 4), i.e., very close to those measured on the purified cytochrome *bc* complex from the Gram-positive *Bacillus* PS3 (Kutoh & Sone, 1988). This corroborates the close relatedness of the cytochrome *bc* complex in the photosynthetic heliobacteria to those operating in respiring representatives of the Firmicutes. The heliobacterial *b*-type cytochromes have E_m values approximately 40 mV lower than those found for the *b_{6f}* complex of higher plants and algae [reviewed in Kallas (1994); for E_m values of *C. reinhardtii* *b_{6f}* complex components, see Pierre et al. (1995)], and about 140 mV lower than those found for the cytochrome *bc₁* complex of *Rb. sphaeroides* [see review by Crofts and Wraight (1983)]. The E_m value of the Rieske 2Fe2S center in *H. mobilis* has been determined previously at $+150$ mV (Liebl, 1993). A number of *c*-type hemes were found to titrate in the range of $+90$ – 180 mV in membrane fragments from *H. mobilis* (Nitschke et al., 1996). The $+120$ mV redox species from this set of hemes is considered to represent the *c*-type cytochrome of the heliobacterial cytochrome *bc* complex [as discussed in Nitschke et al. (1996)].

Light-Induced Redox Changes of *b*-Type Cytochromes. At potentials where the MK pool is oxidized ($E_h > 0$ mV), a small but measurable reduction of cytochrome *b* was observed. A second flash given after a period of time sufficient to re-reduce P_{798}^{+} yielded roughly twice as much reduction of cytochrome *b* than when only one flash was given (not shown). This indicates that, under these conditions, a two-electron-gate mechanism is not involved on the reducing side of the reaction center, or that if such a mechanism does operate, it is in a "scrambled" state in the dark (i.e., approximately half of the gates are in the singly-reduced state, while the others are in the fully oxidized state). Most likely, the one-electron transfer events induced by the light-induced charge separations are equilibrated with the two-electron reduction of MK (ultimately reducing cytochrome *b*) via some ill-determined intermediate electron carriers (such as Fd, NAD^{+}).

Cytochrome *b* behaves similarly at high E_h in higher plant and algal cytochrome *b_{6f}* complexes. In these cases, electrons are introduced into the PQ pool by turnover of photosystem II, and cytochrome *b* is observed to be reduced in the 10–15 ms time scale, followed by a slow reoxidation in the 500–800 ms range. At first glance, the slower

cytochrome *b* oxidation kinetics at high E_h appear to contradict the Q-cycle, since, in this scheme, cytochrome *b* is oxidized at the Q_i site by PQ, which is abundant at high E_h . However, this behavior has recently been reconciled within the framework of a Q-cycle mechanism by assuming that the semiquinone at the Q_i site is relatively unstable in cytochrome *b_{6f}* complexes (Kramer & Crofts, 1992). The cytochrome *bc* complex in *H. mobilis* behaves similarly to cytochrome *b_{6f}* complexes in that cytochrome *b* reduction is quite stable at high E_h , and therefore we conclude that the Q_i site semiquinone in the heliobacterial complex also has a significantly lower stability constant than that of typical cytochrome *bc₁* complexes.

The minimal half-times for reduction of cytochrome *b* at high to moderate E_h were found to be close to 7 ms and titrated with the state of reduction of the MK pool in a way that would be in line with a collisional process between the MK pool and the complex (see Figure 4). In some respects, this behavior is similar to the case in *Rb. sphaeroides*, where interaction of UQH_2 with the Q_o site has been shown to be controlled by a collisional process (Prince & Dutton, 1977; Prince et al., 1978; Meinhardt & Crofts, 1983; Venturoli et al., 1986). However, in purple bacterial chromatophores, flash-induced cytochrome *bc₁* complex turnover appears at ambient potentials significantly above the midpoint potential of the UQ pool (Prince & Dutton, 1977; Prince et al., 1978; Meinhardt & Crofts, 1983), suggesting that the E_m of the UQ/UQH_2 couple bound at the Q_o site has been shifted by preferential binding of UQH_2 [Crofts & Wang, 1989; but see Ding et al. (1992) and references cited within for a contrary view]. In contrast, both the rate and the extent of cytochrome *b* reduction in *H. mobilis* cells closely follow the expected titration of the MK pool [compare Figure 4 with an $E_{m,7}$ for MK of about -60 mV (Kröger & Uden, 1985; Liebl et al., 1992)]. This would indicate that the binding constants for MK and MKH_2 into the *H. mobilis* Q_o site are approximately equal.

Upon lowering the ambient potential, either by progressive anaerobiosis (Figure 3) or by redox poisoning (Figure 5), resulting in the presence of partially reduced cytochrome *b* prior to the flash, a net oxidation of cytochrome *b* was observed. The half-time for the oxidation was about 30–50 ms, and was preceded by a small, transient increase in absorbance, peaking at about 3–5 ms, that we interpret as a reduction in cytochrome *b*. Similar behavior has been observed in chromatophores of *Rb. sphaeroides* (Meinhardt & Crofts, 1983) and spinach thylakoids (Joliot & Joliot, 1986; Moss & Rich, 1987; Kramer & Crofts, 1990) when cytochrome *b_h* was prereduced prior to flash excitation. When reducing conditions were set by the metabolic pathways of the cells, without the addition of mediators, an additional, very slow cytochrome *b* oxidation phase was observed (Figure 3). As the redox potential became lower, this phase was replaced by a more rapid phase of cytochrome *b* oxidation. The slow phase was kinetically similar to cytochrome *b* oxidation under aerobic conditions, which we ascribe to the oxidation of centers with reduced cytochrome *b_h* and oxidized cytochrome *b_l*. This state could have been produced either by multiple turnovers in a fraction of centers or by single turnovers in centers with both *b*-type hemes oxidized prior to the flash excitation. This slow phase was not seen in the presence of mediators, most likely because

equilibration of the redox state of cytochrome *b* with the mediators occurred on a similar time scale.

The redox changes of cytochrome *b* at moderately low E_h can be readily interpreted in the framework of existing Q-cycle models. When cytochrome b_h is prereduced, the MK pool is expected to be predominantly in the MKH₂ form, and the following series of reactions is predicted [see discussion in Meinhardt and Crofts (1983)]. Cytochrome *c* is oxidized by the turnover of the reaction center and, in turn, oxidizes the Rieske iron–sulfur center. Quinol is then oxidized at the Q_o site, transiently reducing cytochrome b_l and releasing a quinone. This quinone can then migrate to a Q_i site and oxidize both cytochrome b_h and cytochrome b_l . The small extent of the cytochrome *b* reduction transient implies that release of quinone, its migration to the Q_o site, and subsequent cytochrome *b* oxidation must be relatively rapid compared to quinol oxidation. The sum of times for quinone release from Q_o and its migration to Q_i was estimated, from kinetic experiments on chromatophores of *Rb. sphaeroides*, to be about 0.5 ms or less (Meinhardt & Crofts, 1983). A similar rate can explain the data in *H. mobilis*.

In *H. mobilis*, under conditions where cytochrome *b* was substantially or completely reduced before the flash, only a net oxidation of cytochrome *b* was observed with a half-time of about 15–20 ms (Figure 3, trace f; Figure 5C, –329 mV trace). This behavior is typical of the cytochrome *b₆f* complexes of higher plants and algae, where an oxidation with a lifetime of about 20 ms following a 2–3 ms lag phase has been reported (Moss & Rich, 1987; Joliet & Joliet, 1986; Kramer & Crofts, 1990, 1995).

Comparative Energetics of Cytochrome *bc* Complexes. The midpoint potential values of cytochrome *b* determined in this work, together with those obtained previously for the MK pool, cytochrome *c*, and the Rieske center (Liebl et al., 1992; Liebl, 1993; Nitschke et al., 1995b, 1996), allow the energetics of cytochrome *bc* turnover to be compared between species. Figure 6 represents a compilation of the changes in free energy upon Q_o site turnover in cytochrome *bc* complexes from four distinct photosynthetic organisms, i.e., *H. mobilis*, *Rb. sphaeroides*, *C. reinhardtii*, and spinach, for the possible steps of electron transfer from QH₂ through the complex and on to the ultimate electron sink, i.e., P⁺. As can be seen in Figure 6, the total Q-cycle free energy changes are strikingly similar in the different species, about +200 mV for each electron transferred from quinol to the reaction center, despite the large differences in quinone redox properties. This probably reflects similar requirements for energy input into proton pumping and subsequent ATP synthesis reactions in all species. A second striking feature illustrated by Figure 6 is the strong conservation of the difference in E_m values between cytochromes b_l and b_h (in the range of 100–130 mV, see steps 2 and 3 in Figure 6).

Figure 6 furthermore reveals two distinct groupings with respect to Q-cycle energetics, classing together the cytochrome *bc* complexes of *Rb. sphaeroides* and *H. mobilis* on one side, and the cytochrome *b₆f* complexes of algae and higher plants on the other side.

In the case of the *Rb. sphaeroides* and *H. mobilis* complexes, quinol oxidation by cytochrome b_l and the Rieske center (step 1) liberates about 10 mV per electron (20 mV total, equivalent to a K_{eq} of approximately 1–10). Each of the following electron transfer steps liberates about 50 mV

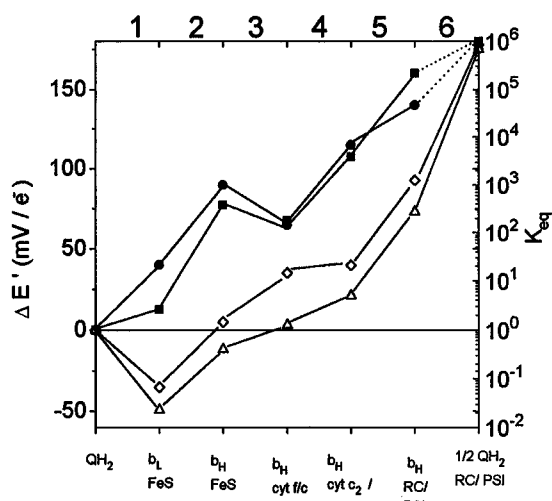
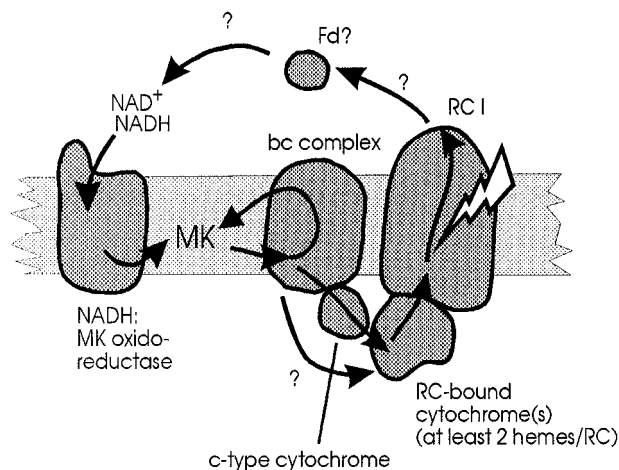


FIGURE 6: Energetic profiles for Q-cycle catalysis by *bc* complexes. Profiles are shown for complexes from *H. mobilis* (closed circles), *Rb. sphaeroides* (closed squares), spinach thylakoids (open diamonds), and *C. reinhardtii* (open triangles). The x-axis is labeled with the high- and low-potential chain components possessing the quinol electrons at each step in the Q-cycle. The $\Delta E'$ values were calculated by the equation: $\Delta E' = \{[E_m(\text{low-chain component}) + E_m(\text{high-chain component})]/2\} - E_m(\text{quinone})$, using E_m values from the literature and this work. The K_{eq} values for these $n = 2$ (i.e., 2 electrons are involved) processes are estimated for room temperature as follows: $K_{eq} \approx 10^{(\Delta E'/30\text{mV})}$. The midpoint potential values for the *Rb. sphaeroides* systems were taken from Crofts and Wraight (1983). For spinach, the E_m values for the 2Fe₂S center, cytochrome b_h , cytochrome b_l , cytochrome *f*, plastocyanin, P₇₀₀, and the PQ pool were taken to be +300 mV (Nitschke et al., 1992), –50 mV (Kramer & Crofts, 1990), –145 mV (Kramer & Crofts, 1990), +360 mV (Rich & Bendall, 1980), +370 mV (Katoh, 1982), +475 mV (Drepper et al., 1996), and +120 mV (Golbeck & Kok, 1979), respectively. For *C. reinhardtii*, the values used were +300 mV (W. Nitschke and D. M. Kramer, unpublished), –84 mV (Pierre et al., 1995), –158 mV (Pierre et al., 1995), +330 mV (Pierre et al., 1995), +365 mV (Kramer, unpublished), and +470 mV (Kramer, unpublished) and +120 mV (Golbeck & Kok, 1979), respectively. Midpoint potential values for *H. mobilis* cytochrome b_h and cytochrome b_l are from this work, and those for the reaction center primary donor, cytochrome c_1 , and cytochrome *c* are taken from Nitschke et al. (1995, 1996).

per electron (K_{eq} of about 100) with the exception of the reduction of cytochrome *c* by the Rieske 2Fe₂S center (step 3). This similarity in energetic profiles for Q-cycle turnover in *H. mobilis* and *Rb. sphaeroides* (the curves deviate by a maximum of only 25 mV per electron) is remarkable in light of the phylogenetic distance between these species and the profound difference in electrochemical properties of the substrate quinones. We consider this to be strong evidence for evolutionary conservation of the basic Q-cycle mechanism between these distant species. As discussed in Nitschke et al. (1995a), this further implies that evolution has “tuned” the electrochemical properties of each redox component of the cytochrome *bc* complex to match the electrochemistry of the donor quinol, and this, in turn, strongly suggests that the specific energetic profile seen in Figure 6 has functional importance.

The cytochrome *b₆f* complexes of higher plants and algae differ from the other types of cytochrome *bc* complexes in key aspects of their energy profiles. First, the reduction of cytochrome b_l and the 2Fe₂S center (step 1) in these complexes appears to be thermodynamically unfavorable (K_{eq} of about 0.1), due to the low E_m of the cytochrome b_l hemes. The extent of free energy released upon each of the

Scheme 1



subsequent electron transfer steps ranges from about 50 to 80 mV, but the total free energy release remains lower than that for the analogous step in the cytochrome *bc* complexes until the final reduction of quinone to quinol at the Q_i site (step 6). Second, in contrast to all other cytochrome *bc* complexes studied, the reduction of the *c*-type cytochrome (cytochrome *f*) by the 2Fe2S center (step 3) appears to be energetically favorable (K_{eq} of about 10). The fact that the energetic profiles of cytochrome *b₆f* complexes from such distinct organisms as *C. reinhardtii* and spinach are so similar again argues in favor of a physiological importance for their specific redox properties.

The Cyclic Electron Transfer Chain of *H. mobilis*. After a saturating single-turnover flash, one positive charge per RC is introduced into the high-potential chain of *H. mobilis*. The primary donor is stoichiometrically reduced by the intermediate cytochrome *c* chain, i.e., the c_{553} hemes [see Nitschke et al. (1995b)], and, in turn, these cytochrome c_{553} hemes are re-reduced by turnover of the cytochrome *bc* complex. Under conditions where all cytochrome *b* is prereduced (see Figure 3, trace *f*), turnover of the cytochrome *bc* complex results in cytochrome *b* oxidation. However, it is clear from Figure 2C that only about 0.25 cytochrome *b* heme was oxidized for each cytochrome *c* that was re-reduced (see Results), despite the fact that roughly stoichiometric amounts of RC and cytochrome *bc* complexes were found (see above). This behavior differs from that observed in chloroplasts of plants or algae, where, under similar conditions, nearly all positive charges introduced into the high-potential chain were transferred to cytochrome *b* (Joliot & Joliot, 1986; Kramer, 1990; Kramer & Crofts, 1993a,b). In order to fully understand the cyclic electron pathway of *H. mobilis*, the fate of these positive charges must therefore be accounted for.

We therefore suggest that the cyclic nature of the *H. mobilis* electron transfer system may account for the data (see Scheme 1). As proposed earlier (Kolpasky et al., 1995), the photosynthetic electron transport cycle in *H. mobilis* would start with charge separation in the RC, resulting in oxidation of MKH_2 in the pool via turnover of the cytochrome *bc* complex. Electrons from the reducing side of the RC complete the cycle by re-reducing the MK pool via an unknown MK reductase, possibly an NADH:MK oxidoreductase. In such a cycle, quinone produced by flash excitation at low E_h can be reduced either at the Q_i site of

the cytochrome *bc* complex, resulting in cytochrome *b* oxidation, or, in competition, at the MK reductase, depending upon the stoichiometries, binding kinetics, and affinities of the respective quinone binding sites. In other words, whereas in spinach thylakoids most of the quinones produced at the Q_o site are re-reduced at the Q_i site, a significant fraction of the MK produced at the Q_o site of the heliobacterial cytochrome *bc* complex may become re-reduced by the quinol reductase, which could, at least in part, explain the relatively small extent of photoinduced cytochrome *b* oxidation. In order to account for the observed differences in behavior between *H. mobilis* on one side and higher plants and algae on the other side, we suggest that PQ molecules released from Q_o sites of cytochrome *b₆f* complexes encounter Q_i sites more readily than Q_B sites, whereas MK released from the Q_o sites of cytochrome *bc* complexes from *H. mobilis* encounter MK reductase sites about as frequently as Q_i sites. This seems reasonable considering the fact that PSII centers are located in the stromal region of the thylakoid and are furthermore shielded by extensive antenna complexes.

Conclusions. In the present study, the electron transport events involving the cytochrome *bc* complex of *H. mobilis*, a photosynthetic representative of the Firmicutes, have been studied *in vivo* and under redox-controlled conditions. The results provide for the first time detailed data on a cytochrome *bc* complex operating in an electron transport chain based on a MK pool. The most obvious conclusion to be drawn from the results described above is the fact that the basic mode of functioning of cytochrome *bc* complexes is conserved between the MK and the UQ/PQ systems. Subtle differences in kinetic details can be rationalized within the concept of current functional models.

With respect to the stability constant of the semiquinone at the Q_i site, the cytochrome *bc* complex in heliobacteria appears to be closely related to cytochrome *b₆f* complexes from cyanobacteria and chloroplasts.

In contrast, the heliobacterial complex differs from cyanobacterial *b₆f* complexes with regard to redox poises during enzyme turnover and resembles typical bacterial cytochrome *bc₁* complexes. The midpoint potentials of the redox centers relative to their respective substrate quinones are conserved between *H. mobilis* and purple bacteria, maintaining the driving forces for quinol oxidation. This suggests a convergent evolution of energy-conserving systems employing different substrate quinones.

Thus, the low E_m values of the *b*-hemes in cytochrome *b₆f* complexes and the resulting low driving force for quinol oxidation appear to be exceptional features in the world of electron transport chains involving cytochrome *bc* complexes. Since low cytochrome *b* heme potentials appear to be conserved across species as diverse as spinach and *C. reinhardtii*, they are likely to be of mechanistic importance to the function of the cytochrome *b₆f* complexes within linear electron transfer chains.

REFERENCES

- Clark, R. D., & Hind, G. (1983) *Proc. Natl. Acad. Sci. U.S.A.* 80, 6249–6253.
- Collins, M. D., & Jones, D. E. (1981) *Microbiol. Rev.* 45, 316–354.
- Cramer, W. A., & Whitmarsh, J. (1977) *Annu. Rev. Plant Physiol.* 28, 132–172.

- Crofts, A. R., & Wraight, C. A. (1983) *Biochim. Biophys. Acta* 726, 149–185.
- Crofts, A. R., & Wang, Z. (1989) *Photosynth. Res.* 22, 69–87.
- DeVries, S., Albracht, S. P. J., Berden, J. A., & Slater, E. C. (1981) *J. Biol. Chem.* 256, 11996–11998.
- Ding, H., Robertson, D. E., Daldal, F., & Dutton, P. L. (1992) *Biochemistry* 31, 3144–3158.
- Drepper, F., Hippler, M., Nitschke, W., & Haehnel, W. (1996) *Biochemistry* 35, 1282–1295.
- Dutton, P. L. (1971) *Methods Enzymol.* 54, 411–435.
- Golbeck, J. H., & Kok, B. (1979) *Biochim. Biophys. Acta* 547, 347–360.
- Gray, K. A., & Daldal, F. (1995) in *The Anoxygenic Photosynthetic Bacteria* (Blankenship, R. E., Madigan, M. T., & Bauer, C. E., Eds.) pp 747–774, Kluwer Academic Publishers, Dordrecht, The Netherlands.
- Hauska, G., Hurt, E., Gabellini, N., & Lockau, W. (1983) *Biochim. Biophys. Acta* 726, 97–133.
- Hiraishi, A. (1989) *Arch. Microbiol.* 151, 378–379.
- Hope, A. B. (1992) *Biochim. Biophys. Acta* 1143, 1–22.
- Hurt, E., & Hauska, G. (1982) *Biochim. Biophys. Acta* 682, 466–473.
- Imhoff, J. F. (1988) in *Green Photosynthetic Bacteria* (Olson, J. M., Ormerod, J. G., Ames, J., Stackebrandt, E., & Trüper, H. G., Eds.) pp 223–232, Plenum Press, New York.
- Joliot, P., & Joliot, A. (1984) *Biochim. Biophys. Acta* 765, 219–226.
- Joliot, P., & Joliot, A. (1986) *Biochim. Biophys. Acta* 849, 211–222.
- Joliot, P., Beal, D., & Frilley, B. (1980) *J. Chim. Phys. Phys.-Chim. Biol.* 77, 209–216.
- Kallas, T. (1994) in *The Molecular Biology of Cyanobacteria* (Bryant, D. A., Ed.) pp 259–317, Kluwer Academic Publishers, Dordrecht, The Netherlands.
- Kato, S. (1982) in *Handbook of Biosolar Resources* (Zaborsky, O. R., Mitsui, A., & Black, C. C., Eds.) Vol. I, Part 1, pp 161–166, CRC Press Inc., Boca Raton, FL.
- Knaff, D. B., & Malkin, R. (1976) *Biochim. Biophys. Acta* 430, 244–252.
- Kolpasky, A., Mühlenhoff, U., Atteia, A., & Nitschke, W. (1995) in *Photosynthesis: From Light to Biosphere* (Mathis, P., Ed.) Vol. II, pp 951–954, Kluwer Academic Publishers, Dordrecht, The Netherlands.
- Kramer, D. M. (1990) Ph.D. Thesis, University of Illinois, Urbana, IL.
- Kramer, D. M., & Crofts, A. R. (1990) in *Current Research in Photosynthesis* (Balscheffsky, M., Ed.) Vol. III, pp 283–286, Kluwer Academic Press, Dordrecht.
- Kramer, D. M., & Crofts, A. R. (1992) in *Research in Photosynthesis* (Murata, N., Ed.) Vol. II, pp 491–494, Kluwer, Dordrecht.
- Kramer, D. M., & Crofts, A. R. (1993a) *Biochim. Biophys. Acta* 1183, 72–84.
- Kramer, D. M., & Crofts, A. R. (1993b) *Biochim. Biophys. Acta* 1184, 193–201.
- Kramer, D. M., & Crofts, A. R. (1995) in *Photosynthesis: From Light to Biosphere* (Mathis, P., Ed.) Vol. II, pp 575–578 Kluwer Academic Publishers, Dordrecht, The Netherlands.
- Kröger, A., & Unden, C. (1985) in *Coenzyme Q* (Lenaz, G., Ed.) pp 285–299, John Wiley and Sons, New York.
- Kutoh, E., & Sone, N. (1988) *J. Biol. Chem.* 263, 9020–9026.
- Liebl, U. (1993) Ph.D. Thesis, University of Regensburg, FRG.
- Liebl, U., Rutherford, A., & Nitschke, W. (1990) *FEBS Lett.* 261, 427–430.
- Liebl, U., Pezennec, S., Riedel, A., Kellner, E., & Nitschke, W. (1992) *J. Biol. Chem.* 267, 14068–14072.
- Meinhardt, S. W., & Crofts, A. R. (1983) *Biochim. Biophys. Acta* 723, 219–230.
- Moss, D. A., & Rich, P. R. (1987) in *Progress in Photosynthesis* (Biggins, J., Ed.) Vol. II, pp 461–465, Martin Nijhoff Publishers, Dordrecht.
- Nitschke, W., & Liebl, U. (1992) in *Research in Photosynthesis* (Murata, N., Ed.) Vol. III, pp 507–510, Kluwer Academic Publishers, Dordrecht, The Netherlands.
- Nitschke, W., Joliot, P., Liebl, U., Rutherford, A. W., Hauska, G., Müller, A., & Riedel, A. (1992) *Biochim. Biophys. Acta* 1102, 266–268.
- Nitschke, W., Kramer, D. M., Riedel, A., & Liebl, U. (1995a) in *Photosynthesis: From Light to Biosphere* (Mathis, P., Ed.) Vol. I, pp 945–950, Kluwer Academic Publishers, Dordrecht, The Netherlands.
- Nitschke, W., Liebl, U., Matsuura, K., & Kramer, D. M. (1995b) *Biochemistry* 34, 11831–11839.
- Nitschke, W., Schoepp, B., Floss, B., Schrick, A., Rutherford, A. W., & Liebl, U. (1996) *Eur. J. Biochem.* 224, 695–702.
- Ohnishi, T., & Trumpower, B. L. (1980) *J. Biol. Chem.* 255, 3278–3284.
- Pace, R. J., Hope, A. B., & Smith, P. (1992) *Biochim. Biophys. Acta* 1098, 209–216.
- Pierre, Y., Breyton, C., Kramer, D., & Popot, J.-L. (1995) *J. Biol. Chem.* 270, 29342–29349.
- Prince, R. C., & Dutton, P. L. (1977) *Biochim. Biophys. Acta* 462, 731–747.
- Prince, R. C., Bashford, C. L., Takamiya, K.-I., van der Berg, W. H., & Dutton, P. L. (1978) *J. Biol. Chem.* 253, 4137–4142.
- Rich, P. R., & Bendall, D. S. (1980) *Biochim. Biophys. Acta* 591, 153–161.
- Riedel, A., Kellner, E., Grodzitzki, D., Liebl, U., Hauska, G., Müller, A., Rutherford, A. W., & Nitschke, W. (1993) *Biochim. Biophys. Acta* 1183, 263–268.
- Robertson, D. E., & Dutton, P. L. (1988) *J. Biol. Chem.* 263, 4137–4142.
- Robertson, D. E., Prince, R. C., Bowyer, J. R., Matsuura, K., Dutton, P. L., & Ohnishi, T. (1984) *J. Biol. Chem.* 259, 1758–1763.
- Sone, N., Sawa, G., Sone, T., & Noguchi, S. (1995) *J. Biol. Chem.* 270, 10612–10617.
- Sone, N., Tsuchiya, N., Inoue, M., & Noguchi, S. (1996) *J. Biol. Chem.* 271, 12457–12462.
- Stackebrandt, E., Murray, R. G. E., & Trüper, H. G. (1988) *Int. J. Syst. Bacteriol.* 38, 321–325.
- Trumpower, B. L. (1990) *J. Biol. Chem.* 265, 11409–11412.
- Venturoli, G., & Zannoni, D. (1988) *Eur. J. Biochem.* 178, 503–509.
- Venturoli, G., Fernandez-Velasco, J. G., Crofts, A. R., & Melandri, B. A. (1986) *Biochim. Biophys. Acta* 935, 258–272.
- Vos, M. H., Klaassen, H. E., & van Gorkom, H. J. (1989) *Biochim. Biophys. Acta* 973, 163–169.
- Wayne, L. G., Brenner, D. J., Colwell, R. R., Grimost, P. A. D., Kandler, O., Krichevsky, M. I., Moore, L. H., Moore, W. E. C., Murray, R. G. E., Stackebrandt, E., Starr, M. P., & Trüper, H. G. (1987) *Int. J. Syst. Bacteriol.* 37, 463–464.
- Yu, J., Hederstedt, L., & Piggot, P. J. (1995) *J. Biol. Chem.* 270, 6751–6760.
- Zannoni, D., & Ingledew, W. J. (1985) *FEBS Lett.* 193, 93–98.